Research Articles

Diagnosing domestic and transboundary sources of fine particulate matter (PM$_{2.5}$) in UK cities using GEOS-Chem

Jamie M. Kelly [a], Eloise A. Marais [a,*], Gongda Lu [a], Jolanta Obszynska [b], Matthew Mace [b], Jordan White [c], Roland J. Leigh [c]

[a] Department of Geography, University College London, Gower Street, London WC1E 6BT, UK
[b] Leicester City Council, Leicester, UK
[c] EarthSense, Leicester, UK

ARTICLE INFO

ABSTRACT

The UK is set to impose a stricter ambient annual mean fine particulate matter (PM$_{2.5}$) standard than was first adopted fourteen years ago. This necessitates strengthened knowledge of the magnitude and sources that influence urban PM$_{2.5}$ in UK cities to ensure compliance and improve public health. Here, we use a regional-scale chemical transport model (GEOS-Chem), validated with national ground-based observations, to quantify the influence of specific sources within and transported to the mid-sized UK city Leicester. Of the sources targeted, we find that agricultural emissions of ammonia (NH$_3$) make the largest contribution (3.7 µg m^{-3} or 38 % of PM$_{2.5}$) to annual mean PM$_{2.5}$ in Leicester. Another important contributor is long-range transport of pollution from continental Europe accounting for 1.8 µg m^{-3} or 19 % of total annual mean PM$_{2.5}$. City sources are a much smaller portion (0.2 µg m^{-3}; 2 %). We also apply GEOS-Chem to the much larger cities Birmingham and London to find that agricultural emissions of NH$_3$ have a greater influence than city sources for Birmingham (32 % agriculture, 19 % city) and London (25 % agriculture, 13 % city). The portion from continental Europe is 16 % for Birmingham and 28 % for London. Action plans aimed at national agricultural sources of NH$_3$ and strengthened supranational agreements would be most effective at alleviating PM$_{2.5}$ in most UK cities.

Introduction

UK ambient pollution of fine particulate matter with aerodynamic diameter < 2.5 µm (PM$_{2.5}$) has steadily declined since the 1970s due mostly to policies targeting large point sources [1]. In the major cities London and Birmingham, PM$_{2.5}$ has decreased by ~4–5 µg m^{-3} over the past decade [2], but still exceeds the recently updated World Health Organization (WHO) annual mean guideline of 5 µg m^{-3} [3]. Long-term exposure to annual mean PM$_{2.5}$ in the UK may account for 29,000–99,000 premature adult deaths each year [4–8]. PM$_{2.5}$ is challenging to regulate, due to a myriad of anthropogenic and natural primary sources, complex chemical and physical processes forming secondary PM$_{2.5}$, and its relatively long lifetime of 1–2 weeks resulting in long-range transport far from the emission source and over national and international regulatory boundaries [9].

Local authorities are tasked with measuring and developing action plans to ensure compliance with regulatory standards in the cities they govern. The standard for annual mean PM$_{2.5}$ is 25 µg m^{-3}; consistent with the EU, but far more lenient than the WHO recommends. Following Brexit, the UK has the autonomy to set its own standards, but an updated PM$_{2.5}$ standard of 10 µg m^{-3} proposed in the Clean Air Strategy published in 2019 [10] has not been implemented. The Clean Air (Human Rights) Bill [11] making its way through the UK Houses of Parliament has defined a PM$_{2.5}$ limit of 10 µg m^{-3} to be met by 1 January 2030. Should this be adopted, the sparsely distributed network of reference measurements of PM$_{2.5}$ in UK cities alone are insufficient to aid local authorities develop strategies to comply with a stricter standard [12].

Chemical transport models (CTMs) that simulate the sources and complex formation, transport, and loss pathways of PM$_{2.5}$ have been used to determine the contribution of individual sources to national and regional PM$_{2.5}$. Vieno et al. (2016b) determined with a high-resolution model (5 km) nested over the UK that a 30 % decrease in individual precursor emissions relative to those emitted in 2010 cause a decline in UK national mean PM$_{2.5}$ from ammonia (NH$_3$) emissions that is 1.5 times greater than that of sulfur dioxide (SO$_2$), 1.6 times greater than primary PM$_{2.5}$, 2.3 times greater than nitrogen oxides (NO$_x$), and 4 times greater

than volatile organic compounds (VOCs). Since 2010, SO_2 emissions have declined by 60 % and NO_x by 33 %, whereas NH_3 emissions have increased by 25 % [13]. Inference of regulatory action from studies that target chemicals rather than specific sources is also limited, as only agriculture overwhelmingly dominates (~90 %) UK anthropogenic NH_3 emissions [14]. The other precursors include a mix of sources currently dominated by road traffic (~30 %) for NO_x, energy industries for SO_2 (~30 %) and residential and commercial small combustion sources (~50 %) for primary $PM_{2.5}$ [13]. Other modelling studies conducted at regional and global scales have also identified the dominant contribution of agricultural emissions of NH_3 to $PM_{2.5}$ pollution [15–17]. Modelling studies have also identified other potentially important transboundary sources of $PM_{2.5}$ in the UK, such as pollution transported from continental Europe [9], the global shipping fleet [18], and dust from the Sahara Desert [19]. The influence of these sources on urban $PM_{2.5}$ pollution in the UK to inform mitigation measures is uncertain.

Observations from national networks and field campaigns have been used to determine the influence of sources within a city on $PM_{2.5}$ pollution. A study quantifying the roadside and urban increments in annual mean $PM_{2.5}$ in London determined that road traffic $PM_{2.5}$ is 50 % more than urban $PM_{2.5}$, mostly due to direct (primary) emissions of $PM_{2.5}$ from vehicle exhausts and non-exhaust emissions from tyre and brake abrasion, but that urban $PM_{2.5}$ is only 18 % more than $PM_{2.5}$ in rural areas surrounding London [20]. Another city source of $PM_{2.5}$ is residential burning of solid biofuels (mostly wood). This source only accounted for 12 % (1.8 µg m^{-3}) of $PM_{2.5}$ pollution in the peak burning season in winter 2010 at an urban site in central London [21]. This source has increased by 35 % since 2010, but remains a relatively small contributor to annual ambient $PM_{2.5}$ [22]. London has 9-times more people and covers an area 6-times greater than the next largest UK city, Birmingham, so the relative contribution of city sources to $PM_{2.5}$ pollution in London may not apply to other UK cities.

The UK city of Leicester, located in the East Midlands 160 km northwest of London, has a population of ~350,000 people; more representative of an average UK city (~217,000 [23] than London (8.9 million). Leicester is among 594 areas in the UK declared Air Quality Management Areas due to routine exceedances of the nitrogen dioxide (NO_2) annual mean standard of 40 µg m^{-3} (https://uk-air.defra.gov.uk/aqma/list; last accessed 13 July 2022). As a result, the local authority targeted road traffic emissions of NO_x [24], due to substantial contribution of traffic to urban NO_2 pollution. Knowledge of the efficacy of similarly targeting city sources is vital for local authorities to develop strategies that address $PM_{2.5}$ pollution in anticipation of a revised standard.

Here we determine the contribution of emissions from select sources and regions to urban $PM_{2.5}$. These include sources within the city limits that could be regulated by local authorities and sources originating outside the city at national, supranational and global scales. We focus on UK cities of distinct sizes: Leicester (73 km^2), Birmingham (270 km^2; 60 km west of Leicester), and London (1,570 km^2). We do this using the GEOS-Chem CTM, following assessment of the model with air quality network measurements distributed throughout the UK and a dense network of low-cost sensors in Leicester.

Methods

The majority of the analysis focuses on 2019 to avoid spurious results associated with dramatic reductions in traffic emissions [25] due to the national lockdown in spring 2020 in response to the COVID-19 pandemic. The low-cost sensors were deployed in a different year, limited to winter (December 2020 to February 2021). This coincides with a second national lockdown, but decline in traffic and other anthropogenic activity was muted in comparison to the first lockdown [26]. We use reference monitor measurements of total $PM_{2.5}$ at the long-term monitoring site in Leicester to assess the potential role of inter-annual variability in meteorology [9] on $PM_{2.5}$ in the two distinct time periods.

The GEOS-Chem chemical transport model

We use GEOS-Chem version 12.1.0 (https://doi.org/10.5281/zenodo.1553349) nested over Europe (32.75°N–61.25°N, 15°W–40°E) at 0.25° × 0.3125° (~25 km latitude × ~31 km longitude), with dynamic (3-hourly) boundary conditions from a global simulation (4° × 5°). The model has 47 vertical levels, extending from the surface to ~80 km and is driven with GEOS-FP assimilated meteorology provided by the NASA Global Modelling and Assimilation Office.

Anthropogenic emissions for the UK are from the National Atmospheric Emission Inventory (NAEI) and those for the rest of Europe are from the European Monitoring and Evaluation Programme (EMEP). Implementation of these in GEOS-Chem is detailed in Marais et al. [14]. In brief, NAEI emissions of NH_3 are increased by 50 % to match satellite-derived estimates [14] and NAEI and EMEP land-based emissions of SO_2 are decreased by a factor of 3 to address large model overestimate in SO_2 concentrations obtained with default EMEP and NAEI emissions compared to surface observations [14]. The NAEI and EMEP emissions are for 2016 and are adjusted in this work to match 2019 conditions using reported annual trends, as is standard [27,28]. These adjustment factors for the prominent gas-phase $PM_{2.5}$ precursors are −2.6 % a^{-1} for NO_x, −3.4 % a^{-1} for SO_2, and −2.0 % a^{-1} for primary $PM_{2.5}$ [13]. No annual scaling is applied to anthropogenic NH_3 emissions, as reported annual changes are small and uncertain [13]. Natural sources of primary $PM_{2.5}$ and precursors of secondary $PM_{2.5}$ are from the Global Emissions InitiAtive (GEIA) inventory [29] for soil and ocean NH_3 and Riddick et al. [30] for seabird NH_3, the Model of Emissions of Gases and Aerosols (MEGAN) version 2.1 [31] for biogenic VOCs, the Dust Entrainment and Deposition (DEAD) scheme for natural dust [32], and the parameterization described in Jaeglé et al. [33] for sea salt.

The model includes coupled gas- and aerosol-phase chemistry to simulate formation of the secondary $PM_{2.5}$ components sulfate (SO_4) [34], nitrate (NO_3) [34], ammonium (NH_4) [34], and secondary organic aerosols (SOA) [35]. In the model, SO_4 is formed irreversibly from gas-phase oxidation of SO_2 by OH, and in-cloud oxidation of SO_2 by ozone (O_3) and hydrogen peroxide (H_2O_2). Ammonia is semi-volatile, so partitions reversibly to acidic aerosols, yielding NH_4 and buffering aerosol acidity [36,37]. If NH_3 is in excess, as is the case in the UK due to controls on SO_2 and NO_x emissions [14], additional NO_3 forms from uptake of nitric acid (HNO_3) generated from oxidation of NO_x. ISORROPIA-II calculates the thermodynamic equilibrium of SO_4-NO_3-NH_4 [38]. Primary OA is represented in the model as organic carbon (OC) and ages with a lifetime of 1.15 days [39]. SOA, represented as OA rather than OC in the model, is estimated with fixed mass yields from precursor emissions of natural and anthropogenic non-methane VOCs (NMVOCs) [35]. The model accounts for dry and wet deposition of gases and aerosols using a resistance-in-series scheme for dry deposition [40,41] and convective scavenging, washout, rainout, entrainment and detrainment for wet deposition [42,43].

Simulated $PM_{2.5}$ concentrations consistent with the measurements, 50 % relative humidity (RH) and ambient temperature and pressure [44], are calculated as the sum of individual components multiplied by representative hygroscopic growth factors:

$$PM_{2.5} = 1.35(SO_4 + NO_3 + NH_4) + BC + 1.07 OAPI + OAPO + 1.86 SSA + DUST \tag{1}$$

DUST is dust with aerodynamic diameter < 2.5 µm, SSA is accumulation-mode sea salt, OAPI is hydrophilic primary and secondary OA, and OAPO is hydrophobic primary OA. The portion of OA simulated by the model as OC is converted to OA for input to Equation (1) using an OA-to-OC ratio of 2.1, representative of aged OA [45].

Contribution of targeted sources to urban PM$_{2.5}$

We use GEOS-Chem to determine the influence of specific sources on urban PM$_{2.5}$ in Leicester, Birmingham and London to aid regulators in identifying effective measures for reducing urban PM$_{2.5}$ pollution. The list of sources we target, summarized in Table 1, includes all sources within the city limits that can be directly regulated by local authorities, sources identified in past studies, as well as exhaust emissions from national road traffic currently regulated to address NO$_2$ pollution to assess whether there are indirect benefits of existing measures. Potentially important sources identified in past studies include the global shipping fleet estimated to account for 10 % of UK PM$_{2.5}$ pollution [18], national agricultural emissions of NH$_3$ [46], anthropogenic emissions from neighbouring countries in continental Europe [9], and dust from uncertain anthropogenic sources [47] and transported from North Africa [19]. For Leicester, we determine the influence of all anthropogenic sources in Leicestershire, due to established coordination of air pollution mitigation strategies between city and county councils. Given the size and proximity of London and Birmingham to Leicester, we also assess the contribution of anthropogenic pollution from these cities to urban PM$_{2.5}$ in Leicester.

We perform 10 model simulations that differ only in the emissions used (Table 2). The base simulation includes all anthropogenic and natural emissions. In the other 9 simulations, individual sources identified in Table 1 are set to zero, so that the difference in PM$_{2.5}$ between the baseline and sensitivity simulations is the PM$_{2.5}$ attributed to the emissions set to zero. This zero-out approach is a standard method for determining the contribution of precursor emissions [48–52,25,8], as non-linearities in annual mean PM$_{2.5}$ are small (<5%) [53,49]. We output monthly means of chemical composition from the model in January to December 2019 following 2 months of model spin-up for chemical initialization and sample model grids overlapping with the extent of the cities of interest (1 grid for Leicester and for Birmingham, 6 grids for London).

Surface measurements

CTMs such as GEOS-Chem include uncertainties in all components of the model that necessitates evaluation against reliable observations to support its use in estimating the influence of city, regional and global PM$_{2.5}$ precursor emissions on urban PM$_{2.5}$ pollution. For this, we use national air quality monitoring network measurements of concentrations of total and components of PM$_{2.5}$ from the Department for Environment, Food, and Rural Affairs (DEFRA) UK-AIR data portal (https://uk-air.defra.gov.uk/data/data_selector, last accessed 16 September 2021). This includes the Automatic Urban and Rural

Table 1
GEOS-Chem sensitivity simulations to assess PM$_{2.5}$ sources in UK cities Leicester, Birmingham, and London.

Simulation	Policy Level	Region	Emission Source	Species [a]
1	City	Leicester	Anthropogenic	All
2	County	Leicestershire	Anthropogenic	All
3[b]	National	London & Birmingham	Anthropogenic	All
4	National	UK	Road Traffic Exhaust	All
5	National	UK	Agriculture	NH$_3$
6	National	UK	Anthropogenic	Dust
7	International	Continental Europe	Anthropogenic	All
8	International	Global	Ships	All
9	International	Global	Natural	Dust

[a] All is anthropogenic NH$_3$, NO$_x$, SO$_2$, BC, OA, dust, and NMVOCs.
[b] Results from simulation 3 are used to assess the contribution of local city sources to PM$_{2.5}$ in London and Birmingham.

Table 2
Baseline total and sensitivity simulation decline in emissions of PM$_{2.5}$ precursors.

Simulation [a]	PM$_{2.5}$ precursor emissions [Gg a^{-1}]					
	SO$_2$	NO$_x$	NH$_3$	BC	OC	Dust
Baseline [b]	63	678	447	13	15	64
1	0.2	2.7	2.2	0.1	0.1	0.3
2	0.8	12	7.9	0.3	0.3	1.0
3	1.3	42	7.2	1.1	1.2	5.7
4	0.4	177	6.6	3.4	3.7	–
5	–	–	384	–	–	–
6	–	–	–	–	–	64
7	193	1909	1092	55	95	103
8	398	2421	0.2	33	17	109[c]
9	–	–	–	–	–	602

[a] Sensitivity simulation numbers correspond to those detailed in Table 1. Values for simulations 1–9 are the difference between the baseline and sensitivity simulation emissions for the nested domain (Section 2.1).
[b] Total anthropogenic and natural emissions for the UK National Atmospheric Emission Inventory domain that includes UK territorial waters and scaling factors implemented in GEOS-Chem (Section 2.1). Percent contribution of anthropogenic emissions to total UK emissions: 72% for NO$_x$, 87% for SO$_2$, 95% for NH$_3$, 92% for BC, and 93% for OC.
[c] Dust as surrogate for ash.

Network (AURN) of ratified hourly reference measurements of total PM$_{2.5}$ concentrations across 72 sites classified as urban (38 sites), urban traffic (23), industrial (5), rural (4 sites), and suburban (2), and the UK Eutrophying and Acidifying Pollutants (UKEAP) network of monthly mean concentrations of the PM$_{2.5}$ components NH$_4$, SO$_4$ and NO$_3$ at 18 rural sites. The UKEAP measurement technique and consistency with other measurements are detailed in Tang et al. [54]. The rural Auchencorth Moss site in Scotland, south of Edinburgh, includes UKEAP measurements of SO$_4$, NO$_3$, and NH$_4$, as well as elemental carbon (EC) (that we use to assess simulated black carbon or BC) and organic carbon (OC). EC and OC are weekly measurements made with a thermal/optical carbon analyser [55]. Annual means are only estimated at sites with temporal coverage of at least 75 % for total PM$_{2.5}$ and at least 65 % for components of PM$_{2.5}$. Increasing the temporal data coverage threshold by 10 percentage points has negligible effect on the annual means. Locations of relevant measurement sites are shown in Section 3. Some model grid cells contain multiple measurement sites, which we do not average, as this artificially improves the model-measurement statistics.

The single GEOS-Chem grid that overlaps with Leicester is evaluated against a single AURN PM$_{2.5}$ site in the city. Given this, we use PM$_{2.5}$ data from a network of low-cost sensors distributed throughout Leicester to assess consistency between monthly mean PM$_{2.5}$ measured at the AURN site and averaged across all low-cost sensor sites. The network includes 19 EarthSense Zephyr® optical particle counters covering 7 size bins from 0.3 to 10 μm diameter with a 10-second sampling frequency. Particulate number concentrations are converted to mass concentrations using number density and volume representative of each size bin and the sum of the mass ≤ 2.5 μm used to calculate PM$_{2.5}$. The well-known positive bias in low-cost sensor PM$_{2.5}$ due to aerosol water from hygroscopic growth of particles [56] is mitigated with the Zephyrs by internal heating of the sampling cavity to reduce humidity prior to sampling. Any remaining high bias due to aerosol water is addressed with an interaction term between PM$_{2.5}$ and RH as is now a standard approach to improve sensor accuracy for instruments that retrieve aerosol mass with light scattering techniques [57–59].

Results and discussion

Spatial variability and seasonality of PM$_{2.5}$ across the UK

Fig. 1 compares observed (AURN) annual mean PM$_{2.5}$ at individual sites to coincident gridboxes of simulated annual mean PM$_{2.5}$ across the
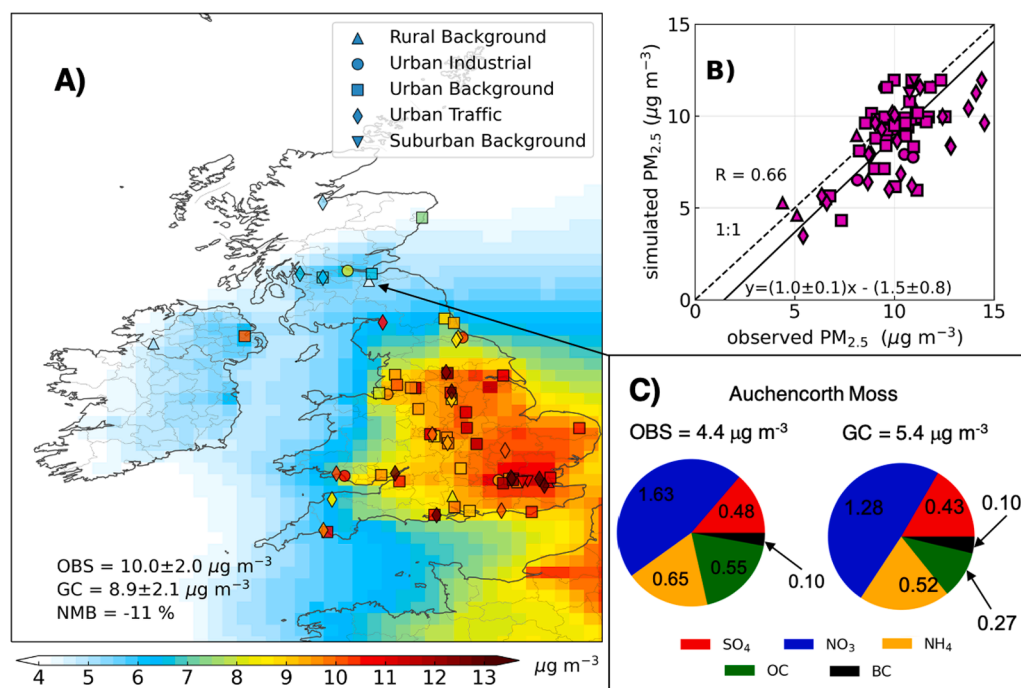
Fig. 1. Comparison of observed and simulated annual mean PM$_{2.5}$ in 2019. Panels are (A) mapped observed (filled shapes) and modelled (background) total PM$_{2.5}$, (B) regression of individual site measurements and coincident model grids, and (C) PM$_{2.5}$ composition at Auchencorth Moss for measured components of PM$_{2.5}$. OC is compared instead of OA due to uncertainties in converting measured OC to OA. Shapes in (A) and (B) discern site types. Values inset are the observed (OBS) and modelled (GC) annual means and model normalized mean bias (NMB) in (A), the Pearson's correlation coefficient and reduced major axis (RMA) regression equation in (B), and mass concentrations of total PM$_{2.5}$ above each pie and select components of PM$_{2.5}$ for each piece of the pie in (C). Lines in (B) are the 1:1 relationship (dashed) and RMA regression (solid). Slope and intercept errors are obtained with bootstrapping.

UK. The total UK emissions of PM$_{2.5}$ precursors in the model are given in Table 2. The mean of all AURN sites in Fig. 1 is 10 μg m^{-3}, and ranges from 4 μg m^{-3} at the Auchencorth Moss rural site in Scotland to 15 μg m^{-3} at urban traffic sites on Marylebone Road in London and Barnsley Road in Sheffield. In cities with a mix of urban and rural sites (London, Southampton and Edinburgh), urban PM$_{2.5}$ is just 1.5–2.0 μg m^{-3} (or 20–50 %) more than rural PM$_{2.5}$, reflecting the large influence of sources originating from outside the city [20]. The model captures the observed spatial pattern (r = 0.66) and variance (regression slope = 1.0 ± 0.1), but exhibits a low bias (normalized mean bias of NMB = -11 %) that is due to a 1.5 ± 0.8 μg m^{-3} underestimate in PM$_{2.5}$ (negative intercept in Fig. 1B). The model bias is greatest (NMB = -18 %) for urban traffic sites and is to be expected, as the influence of city sources on the measurements is diluted at the model resolution of 25–31 km. No measurements or model grids exceed the current standard of 25 μg m^{-3}, whereas the WHO annual mean guideline of 5 μg m^{-3} is exceeded at all but 1 AURN site and all but 2 of the model grids coincident with the sites. Of all simulated UK grids, 79 % exceed the updated guideline.

Fig. 1 also compares the measured and modelled components of PM$_{2.5}$ at Auchencorth Moss. The measured components are 78 % of total PM$_{2.5}$ mass (91 % if OC is converted to OA using an OA-to-OC ratio of 2.1). The dominant measured component of PM$_{2.5}$ is NO$_3$ (accounting for 37 % of PM$_{2.5}$), followed by NH$_4$ (15 %), OC (13 %), SO$_4$ (11 %), and BC (2 %). Generally, the model captures the observed order of importance, except for OC. In the model, the order is 23 % NO$_3$, 9 % NH$_4$, 8 % SO$_4$, 5 % OC, and 2 % BC summing to 47 %. The remaining modelled PM$_{2.5}$ is dust (21 %), aerosol liquid water (19 %), and sea salt (<5 %). The large model underestimate for OC (-50 %) occurs in all seasons and is consistent with low model biases in OC across Europe from multiple CTMs [60] attributed to underestimated biogenic and anthropogenic SOA. The model exhibits a positive 23 % bias in total PM$_{2.5}$ at the site, but negative bias for the measured components SO$_4$ (-10 %), NO$_3$ (–22 %), and NH$_4$ (-20 %). This points to a model overestimate in either dust, sea salt or aerosol water. Simulated annual mean dust PM$_{2.5}$ is 1.1 μg m^{-3}, accounting for a large portion (21 %) of the simulated total PM$_{2.5}$. This may be erroneous, as emissions of anthropogenic dust are uncertain [47]. The model overestimate in dust is at least a factor of ~3, using the difference between measured total and the sum of the components of PM$_{2.5}$ as an upper limit estimate of dust PM$_{2.5}$. The cause is most likely

an overestimate in sources rather than transport or loss processes, supported by consistency between modelled and observed BC, as BC abundance depends also on emissions, transport and loss processes dominated by wet scavenging [61]. According to our model sensitivity simulations (Table 1), 70 % of PM$_{2.5}$ dust at Auchencorth Moss is from anthropogenic sources totalling 64 Gg a^{-1} in GEOS-Chem (Table 2).

Fig. 2 compares observed and simulated concentrations of secondary inorganic aerosol components at rural UKEAP sites. Network mean observed values of SO$_4$ (0.58 μg m^{-3}), NO$_3$ (1.78 μg m^{-3}) and NH$_4$ (0.75 μg m^{-3}) are similar to those measured at Auchencorth Moss (Fig. 1C). The model captures the observed spatial distribution of all 3 components (r = 0.72–0.85) and variance of NO$_3$ and NH$_4$ (slope = 0.8–0.9). The underestimate in modelled SO$_4$ variance (slope = 0.6 ± 0.1) may reflect overcorrection of the SO$_2$ emissions (Section 2.1), particularly for model grids influenced by large point sources of SO$_2$ in northeast England. The mean underestimate in modelled SO$_4$ is 19 %. Because NH$_3$ is in excess of acidic aerosols in the UK, formation of NH$_4$ depends on abundance of SO$_4$ rather than abundance of NH$_3$. As a result, the low model bias in SO$_4$ contributes to model underestimate in the acid buffer NH$_4$ that in turn contributes to a slight (15 %) underestimate in modelled NO$_3$ (12 %). Also because NH$_3$ is in excess, the emissions scaling applied to NH$_3$ to resolve differences between top-down and bottom-up emissions estimates (Section 2.1) has limited effect on NH$_4$ and PM$_{2.5}$. Most of this additional NH$_3$ settles to the Earth's surface via dry and wet deposition.

Fig. 3 assesses simulated seasonality of total and secondary inorganic PM$_{2.5}$ concentrations. These peak in spring (March-May) and are at a minimum in summer (June-August). Total PM$_{2.5}$ ranges from ~20 μg m^{-3} in April to ~7.5 μg m^{-3} in August. The spring peak is due to a combination of mild temperatures enhancing partitioning of gas phase precursors into the aerosol phase, easterlies importing pollution from mainland Europe, stagnant conditions over the UK limiting ventilation, and a peak in NH$_3$ emissions due to March-April fertilizer application [62,63,9,64]. The model captures the observed seasonal cycle in PM$_{2.5}$, but with a year-round underestimate averaging just under 1 μg m^{-3} that is consistent with the range of the regression intercept (-1.5 ± 0.8 μg m^{-3}) in Fig. 1B. The model underestimate in Fig. 3 is larger (1–2 μg m^{-3}) in summer when SO$_4$, NO$_3$ and NH$_4$ are all underestimated (Fig. 3B). This summertime underestimate may be due to a larger summertime underestimate in bottom-up NH$_3$ emissions than the rest of the year that
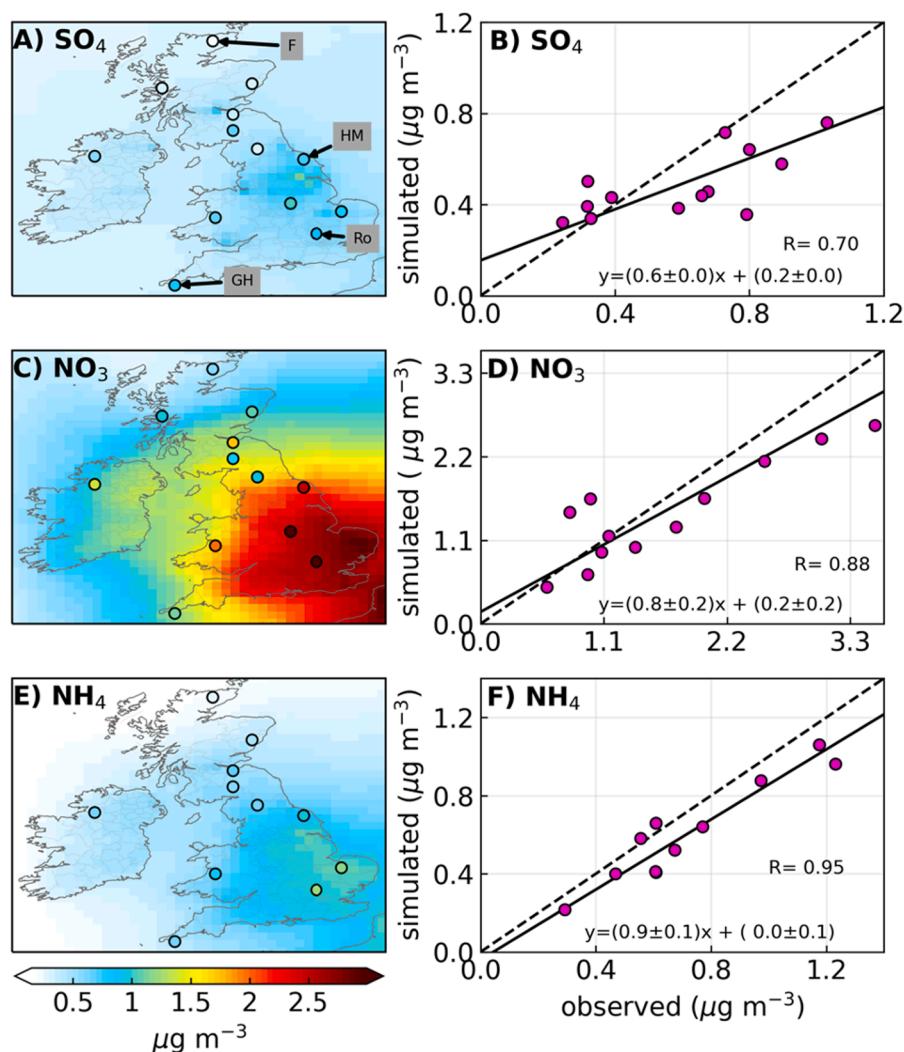
Fig. 2. Evaluation of simulated annual mean secondary inorganic PM$_{2.5}$ components. Panels compare mapped observed (filled circles) and modelled (background) SO$_4$ (top), NO$_3$ (middle), and NH$_4$ (bottom) (A, C, E) and regression of the two (B, D, F). Lines are 1:1 relationships (dashed) and RMA regressions (solid). Inset values are observed (OBS) and modelled (GC) annual means, model normalized mean biases (NMB), Pearson's correlation coefficient (r), and RMA regression equations. Slope and intercept errors are obtained with bootstrapping. Locations of sites used to assess seasonality of SO$_4$, NO$_3$, and NH$_4$ in Fig. 3 (Goonhilly (GH), Rothamsted (Ro), High Muffles (HM), and Forsinard (F)) are indicated in (A).
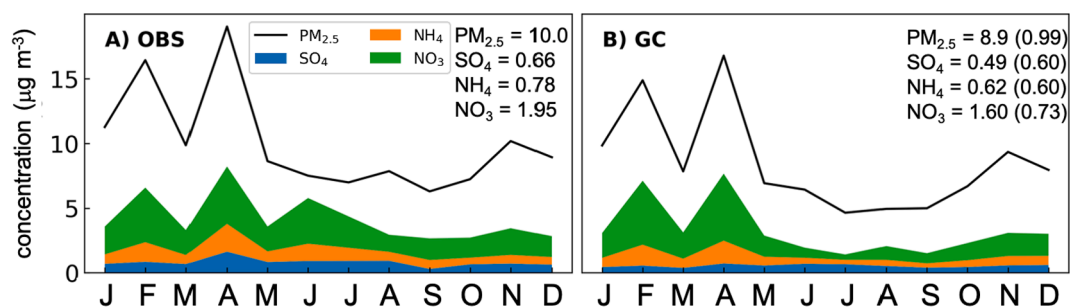
Fig. 3. Seasonality in total and secondary inorganic PM$_{2.5}$ components across the UK. Panels are time series of (A) observed and (B) modelled monthly mean total (black line) and secondary inorganic aerosol components (colored filled stacks: blue for SO$_4$, orange for NH$_4$, green for NO$_3$). Observations are from all AURN sites shown in Fig. 1A and select UKEAP sites from Fig. 2A where sample collection occurs at or close to the start and end of the month (see text for details). Values inset are annual means of the observations in (A) and model in (B) and, in parentheses, the temporal correlation (Pearson's correlation coefficient) in (B) between the measurements and model for the total and components of PM$_{2.5}$. (For interpretation of the references to colour in this figure legend, the reader is referred to the web version of this article.)

has been identified from comparison to top-down satellite-derived NH$_3$ emissions [14]. Slow conversion of SO$_2$ to sulfate in CTMs may also contribute to the summer low bias [65].

Domestic and distant source contributions to UK-wide PM$_{2.5}$

We use the model to identify the relative contribution of individual sources (Table 1) to UK-wide PM$_{2.5}$, given the ability of the model to reproduce the variance and seasonality in annual mean total PM$_{2.5}$ (Figs. 1 and 3) and the dominant components SO$_4$, NO$_3$, and NH$_4$ (Figs. 1 and 2). The emissions totals for PM$_{2.5}$ precursors are given in Table 2. Compared to national emissions, the contribution of Leicester and Leicestershire precursor emissions is < 1 %, road traffic NO$_x$ is 26 % of total NO$_x$, and agriculture 86 % of total NH$_3$. The spatial distribution of the

influence of the sources targeted on annual mean total $PM_{2.5}$ are shown in Fig. 4. Of the sources targeted, national agriculture has the greatest influence (2.2 µg m^{-3} or 32 % of UK annual mean total $PM_{2.5}$), followed by UK anthropogenic dust (1.1 µg m^{-3} or 16 %) and transboundary anthropogenic pollution from continental Europe (1.4 µg m^{-3} or 20 %). The influence of agriculture on UK $PM_{2.5}$ may be conservative, as the model underestimates annual mean NH_4 (Fig. 2E, Section 3.1) and summertime $PM_{2.5}$ (Fig. 3, Section 3.1). Elevated concentrations of $PM_{2.5}$ are regionally distributed over most of England for agriculture, and across the English Channel for transboundary sources. Anthropogenic dust $PM_{2.5}$ peaks in cities, as urban sources are dominant, according to the model, though there may be a potentially large positive bias in anthropogenic dust emissions in the model (Section 3.1). Seasonality in the key contributors, UK agriculture and transboundary pollution from Europe, shown as monthly means in Fig. 5, ranges from < 1 µg m^{-3} in summer to 5–6 µg m^{-3} in spring. The other sources (UK traffic, global ships, and natural desert dust) have similar annual contributions of 0.5–1.0 µg m^{-3} (6–9 %) and also peak in spring, but at < 2 µg m^{-3}.

Interannual variability in meteorology impacts the relative influence of transboundary sources of $PM_{2.5}$ in the UK. At a rural monitoring site in the UK, for example, the annual contribution of all non-UK sources to SO_4 and NO_3 aerosol mass varied from 20 to 90 % in 2001 to 2010 [9] due to shifts in meteorology [9]. According to the annual status report of UK climate [66], 2019 was 5 % warmer than the climatological (1981–2010) mean, mostly because February was 2–3 °C warmer. Rainfall in 2019 exceeded average conditions by 7 %, ranging from unusually dry in winter to unusually wet the rest of the year. The dry conditions in winter were associated with a higher-than-normal pressure system over the UK and the western portion of mainland Europe that favoured transport of air from mainland Europe. This transport pattern was sustained in most of spring [66] and suggests that the 2019 contribution of anthropogenic pollution from Europe in winter and spring (Fig. 5) was more than normal. Regardless, the annual $PM_{2.5}$ contributions we obtain in 2019 using GEOS-Chem are broadly consistent with results from other models targeting different years. Specifically, 33 % from agriculture in 2010 [46,16], 20 % from transboundary sources in 2003 [9], and < 5 % from traffic in 2021 [20].
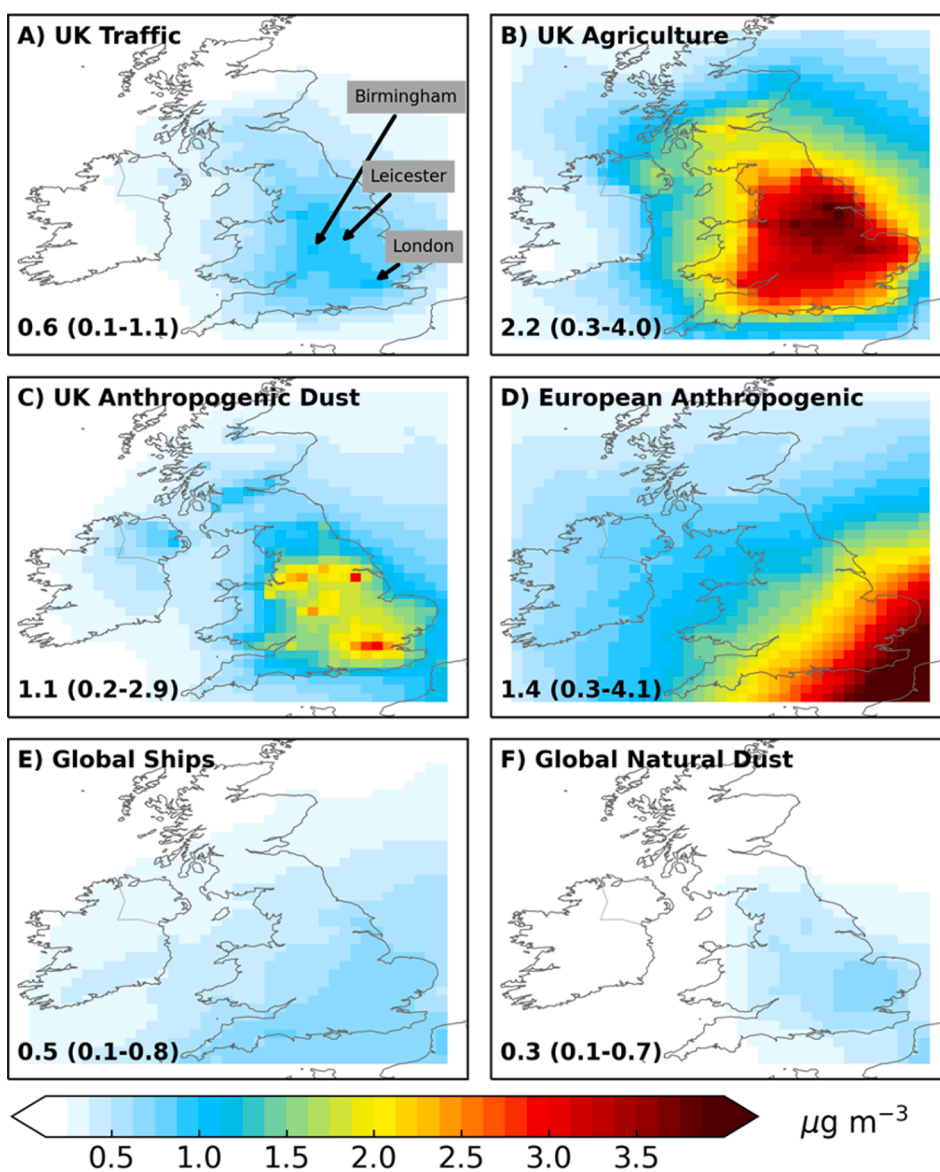

Fig. 4. Spatial distribution of simulated source contributions to annual mean total $PM_{2.5}$ concentrations. These are (A) traffic, (B) agriculture, (C) anthropogenic dust, (D) continental Europe, (E) ships, and (F) natural dust (see Table 1 for details). Inset values are UK means and, in parentheses, ranges (min to max) for UK land grids. Locations of Leicester, Birmingham, and London city centres are indicated in A.
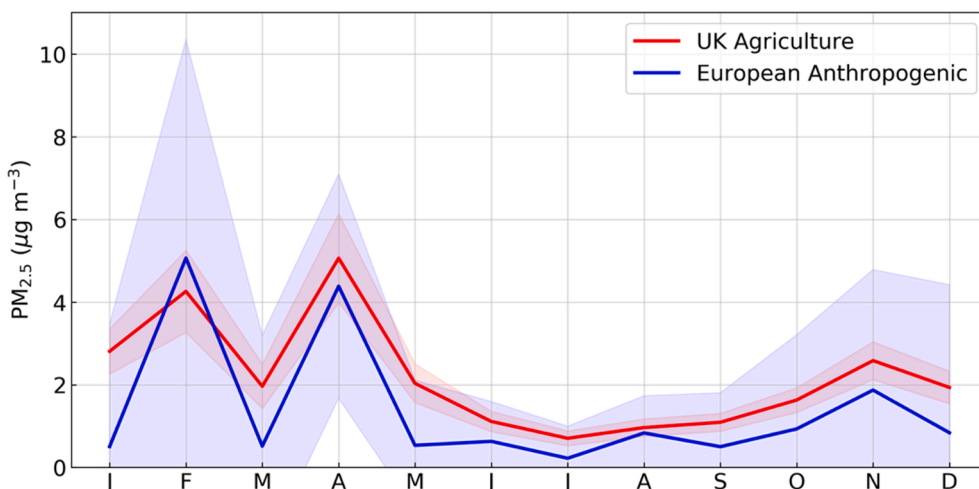
Fig. 5. Seasonality in UK mean PM$_{2.5}$ from dominant sources agriculture and continental Europe. Solid lines are monthly mean PM$_{2.5}$ from UK agriculture (red) and European anthropogenic sources (blue). Shading indicates spatial variability ($\pm 1\sigma$ standard deviation). (For interpretation of the references to colour in this figure legend, the reader is referred to the web version of this article.)

Sources of PM$_{2.5}$ pollution in Leicester, London and Birmingham

According to GEOS-Chem, annual mean PM$_{2.5}$ was 9.5 µg m^{-3} in Leicester in 2019; 17 % less than 11.4 µg m^{-3} measured at the urban AURN site in Leicester. This is consistent with the model NMB obtained from comparison to all AURN sites (Fig. 1). Fig. 6 shows the contribution of individual sources to simulated total and components of PM$_{2.5}$ in Leicester. The sum of all sources targeted (11.4 µg m^{-3}) exceeds the annual mean due to overlap in source locations (city, county, national) and interdependence of sources. The latter includes dependence of NO$_3$ formation from NO$_x$ emissions on agricultural NH$_3$ emissions that causes the 45 % mass contribution of NO$_3$ for PM$_{2.5}$ from agricultural emissions of NH$_3$ in Fig. 6. The contribution of national agriculture is largest at 3.7 µg m^{-3} (39 %), as expected from its widespread influence over England (Fig. 4). Transboundary pollution from continental Europe contributes 1.8 µg m^{-3} (19 %). In spring, the monthly contribution from each of these sources can exceed 6 µg m^{-3}. Anthropogenic dust is slightly more than long-range transport from Europe, but emission estimates of this

source are uncertain and lack of direct observations of surface concentrations of dust prevents validation of GEOS-Chem. Only 0.2 µg m^{-3} or 2 % of total PM$_{2.5}$ is due to all city sources, and only 1.0 µg m^{-3} (11 %) to all county sources. London and Birmingham together contribute 0.4 µg m^{-3}; double that from all sources in Leicester.

Traffic exhaust emissions, one of the most regulated sources in the UK due to the impact on NO$_2$ pollution, is only 1.0 µg m^{-3} (11 %) of Leicester PM$_{2.5}$ pollution. This is only 0.4 µg m^{-3} more than the contribution from distant ship traffic (0.3 µg m^{-3}; 6 %). NO$_3$ is the dominant component from ship emissions, so this source contribution should steadily decline due to an anticipated 4 % a^{-1} decrease in shipping NO$_x$ emissions from stricter controls on emissions from new ships [67].

Uncertainties in the simplistic scaling factors we apply to NH$_3$ and SO$_2$ emissions have limited effect on the contribution of targeted sources to concentrations of PM$_{2.5}$ in Fig. 6. Most of the additional UK-wide 50 % increase in NH$_3$ emissions deposits to the surface of the Earth via dry and wet deposition, as formation of NH$_4$ is limited by availability of acidic
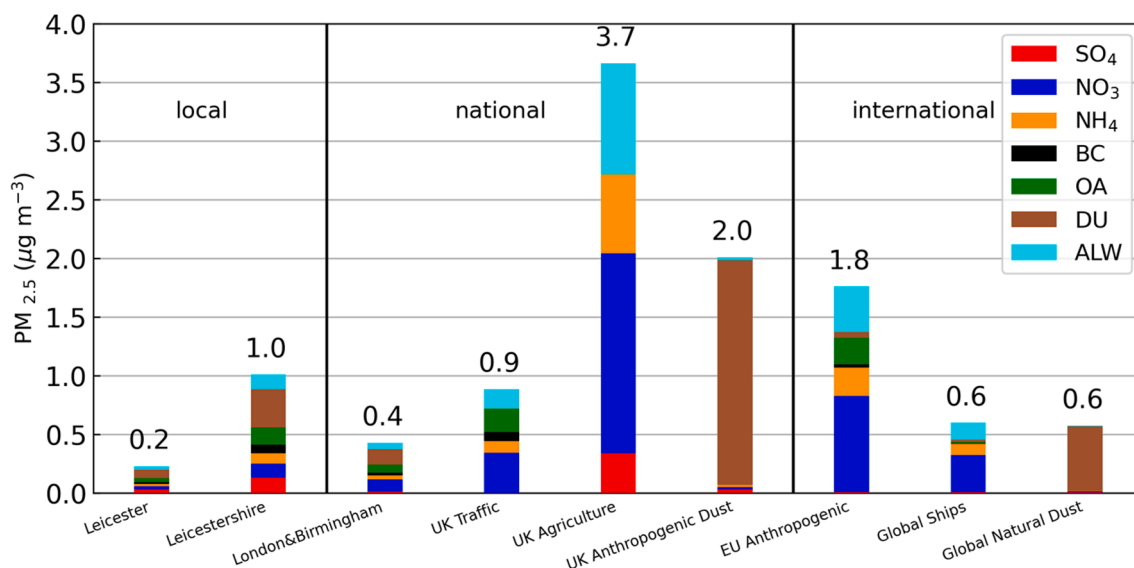

Fig. 6. Source contributions to annual mean total and components of PM$_{2.5}$ in Leicester. These are obtained as the difference between baseline and sensitivity simulations (Table 1). Bar colors distinguish the PM$_{2.5}$ components SO$_4$ (red), NO$_3$ (blue), NH$_4$ (orange), BC (black), OA (green), dust (brown), and aerosol liquid water (ALW) (cyan). Solid vertical lines separate local, national, and international sources (see Table 1 for details). (For interpretation of the references to colour in this figure legend, the reader is referred to the web version of this article.)
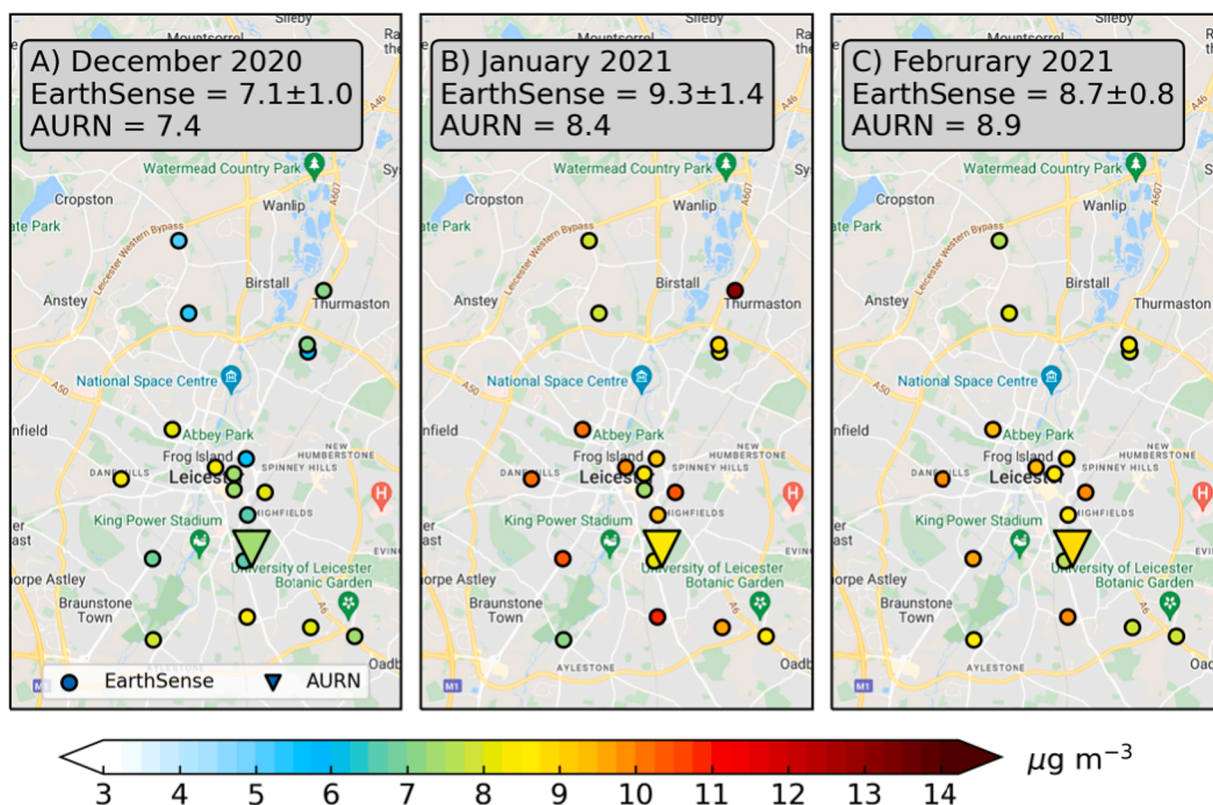
Fig. 7. Monthly mean PM$_{2.5}$ concentrations in Leicester from EarthSense low-cost sensors (circles) and AURN (upside down triangle). Values inset are the monthly mean and spatial variability ($\pm 1\sigma$ standard deviation) across the low-cost network and the monthly mean at the AURN site.

aerosols in the UK [14]. If we had applied the original NAEI SO$_2$ emissions to GEOS-Chem and if we account for the influence of this additional SO$_2$ on SO$_4$, NO$_3$ and NH$_4$, the city sources contribution to PM$_{2.5}$ would be at most ~0.09 µg m^{-3} more secondary inorganic aerosols and ~0.03 µg m^{-3} more associated aerosol liquid water than is shown in Fig. 6. This would lead to 3 % rather than 2 % contribution of city sources to Leicester PM$_{2.5}$.

Fig. 7 shows the distribution of monthly mean observed PM$_{2.5}$ across Leicester in December 2020 to February 2021 from the Zephyr® network of low-cost sensors. Network mean PM$_{2.5}$ is 8.4 ± 0.6 µg m^{-3}

during the measurement period, similar to the Leicester AURN site mean of 8.2 µg m^{-3}. This suggests that PM$_{2.5}$ at this site is representative of mean PM$_{2.5}$ for the city and so is appropriate for assessing GEOS-Chem simulation of Leicester PM$_{2.5}$ pollution. Two low-cost sensors are missing in February 2021, but the network is dense enough that, when these two sites are excluded, network mean PM$_{2.5}$ changes by 1 % in December 2020 and 3 % in January 2021. PM$_{2.5}$ measured at the Leicester AURN site in winter months in 2019 (the target year for GEOS-Chem simulations) is 50 % more than it is in December 2020 to February 2021 (the low-cost sensor measurement period). This is likely because
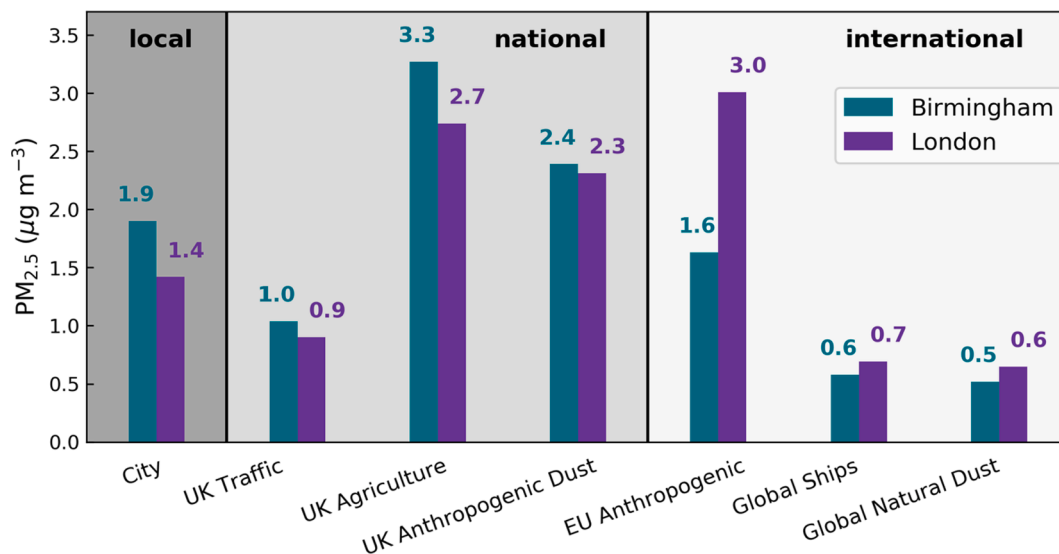

Fig. 8. Source contributions to annual mean PM$_{2.5}$ in Birmingham (green) and London (purple). Shading and vertical lines distinguish local, national, and international sources (see Table 1 for details). (For interpretation of the references to colour in this figure legend, the reader is referred to the web version of this article.)

the meteorological conditions in January-February 2019 promoted long-range transport of pollution from continental Europe (Section 3.2).

In Fig. 8, we extend application of GEOS-Chem to Birmingham and London to determine the contribution of all but the county-level sources to $PM_{2.5}$ in these cities. According to the model, annual mean $PM_{2.5}$ in 2019 was 10.1 μg m^{-3} in Birmingham (0.6 μg m^{-3} more than Leicester) and 10.9 μg m^{-3} in London (1.4 μg m^{-3} more than Leicester). The model values are similar to the city mean of the AURN sites in Birmingham (9.6 μg m^{-3}) and the same as those in London (10.9 μg m^{-3}). All three cities have similar contributions from natural dust (0.5–0.6 μg m^{-3}), traffic (0.9–1.0 μg m^{-3}), and ships (0.6–0.7 μg m^{-3}). Agriculture is 0.4 μg m^{-3} less, anthropogenic dust 0.4 μg m^{-3} more, and city sources 1.7 μg m^{-3} more for Birmingham than for Leicester. Due to the proximity of London to continental Europe, the contribution from European pollution (Fig. 4) in London is 28 %; 1.2 μg m^{-3} more than Birmingham and 1.4 μg m^{-3} more than Leicester. London city sources are 1.2 μg m^{-3} more and agriculture 1.0 μg m^{-3} less than these are in Leicester. The relative contribution of city sources we obtain for London of 13 % is less than the 18 % inferred from differences in urban and rural measurements of total $PM_{2.5}$ [20]. The city source contribution increases to 24 % for the model grid overlapping with Central London.

Conclusions

In this study, we quantified the influence of targeted emission sources on urban $PM_{2.5}$ in the UK using the GEOS-Chem chemical transport model validated with UK-wide measurements of total and components of $PM_{2.5}$ and a dense network of low-cost sensors of total $PM_{2.5}$ in the mid-sized UK city Leicester. According to the model, 79 % of the UK exceeds the new WHO guideline of 5 μg m^{-3}. Across the size gradients of cities investigated, from Leicester to Birmingham to London, our results suggest that city sources for almost all cities in the UK account for considerably less than 20 % of $PM_{2.5}$ pollution. Addressing $PM_{2.5}$ pollution in cities to meet an anticipated stricter standard and improve public health would require a shift from local action plans to national-scale measures focusing on agricultural sources of ammonia (NH_3) that account for 25–39 % of urban $PM_{2.5}$ pollution and ongoing and strengthened internationally agreed regulations to reduce long-range transport of pollution from continental Europe that accounts for 16–28 % of urban $PM_{2.5}$ pollution. The ability to reliably estimate the influence of anthropogenic dust sources on urban $PM_{2.5}$ is impeded by lack of observations to quantify, diagnose and address biases likely originating from uncertain emissions.

Data Availability

The GEOS-Chem data generated and used in this study are available from the UCL Data Repository (https://doi.org/10.5522/04/20305401). Access to the low-cost sensor $PM_{2.5}$ data can be requested from Matthew Mace (Matthew.Mace@leicester.gov.uk).

Author Contributions

EAM is responsible for project conceptualisation and performed all model simulations. JMK analysed all model and most observation data, with input from GLu. JW and RJL provided the low-cost sensor data. Low-cost sensors were deployed in Leicester by JL and MM. JL, MM, and EAM acquired funding. JMK and EAM wrote the manuscript, with editorial input from JW, RJL, JL, and MM.

Declaration of Competing Interest

The authors declare that they have no known competing financial interests or personal relationships that could have appeared to influence the work reported in this paper.

Data availability

GEOS-Chem data are available from the UCL Data Repository (https://doi.org/10.5522/04/20305401). Access to low-cost sensor data can be requested from Matthew Mace (Matthew.Mace@leicester.gov.uk).

References

[1] Carnell E, Vieno M, Vardoulakis S, Beck R, et al. Modelling public health improvements as a result of air pollution control policies in the UK over four decades-1970 to 2010. Environ Res Lett 2019;14:12. https://doi.org/10.1088/1748-9326/ab1542.

[2] Vohra K, Marais EA, Suckra S, Kramer L, et al. Long-term trends in air quality in major cities in the UK and India: a view from space. Atmos Chem Phys 2021;21:6275–96. https://doi.org/10.5194/acp-21-6275-2021.

[3] WHO. WHO global air quality guidelines: particulate matter ($PM_{2.5}$ and PM_{10}), ozone, nitrogen dioxide, sulfur dioxide and carbon monoxide; 2021. Available: https://apps.who.int/iris/handle/10665/345329 [Accessed 12-04-2022].

[4] Committee on the Medical Effects of Air Pollutants. The Mortality Effects of Long-Term Exposure to Particulate Air Pollution in the United Kingdom; 2010. Available: https://assets.publishing.service.gov.uk/government/uploads/system/uploads/attachment_data/file/304641/COMEAP_mortality_effects_of_long_term_exposure.pdf [Accessed 12-04-2022].

[5] Public Health England. 2014. Estimating Local Mortality Burdens associated with Particulate Air Pollution. Available: https://assets.publishing.service.gov.uk/government/uploads/system/uploads/attachment_data/file/332854/PHE_CRCE_010.pdf [Accessed 11-04-2022].

[6] Lelieveld J, Klingmuller K, Pozzer A, Poschl U, et al. Cardiovascular disease burden from ambient air pollution in Europe reassessed using novel hazard ratio functions. Eur Heart J 2019;40:1590–6. https://doi.org/10.1093/eurheartj/ehz135.

[7] Fenech S, Doherty RM, O'Connor FM, Heaviside C, et al. Future air pollution related health burdens associated with RCP emission changes in the UK. Sci Total Environ 2021;773:13. https://doi.org/10.1016/j.scitotenv.2021.145635.

[8] Vohra K, Vodonos A, Schwartz J, Marais EA, et al. Global mortality from outdoor fine particle pollution generated by fossil fuel combustion: Results from GEOS-Chem. Environ Res 2021;195. https://doi.org/10.1016/j.envres.2021.110754.

[9] Vieno M, Heal MR, Hallsworth S, Famulari D, et al. The role of long-range transport and domestic emissions in determining atmospheric secondary inorganic particle concentrations across the UK. Atmos Chem Phys 2014;14:8435–47. https://doi.org/10.5194/acp-14-8435-2014.

[10] DEFRA. Clean Air Strategy 2019; 2019. Available: https://www.gov.uk/government/publications/clean-air-strategy-2019 [Accessed 12-4-2022].

[11] Clean Air (Human Rights) Bill 2022 (HL Bill no. 69). Available from: https://bills.parliament.uk/publications/48605/documents/2487 [Accessed 5 December 2022].

[12] United Nations Economic Comission for Europe. Emission Reduction Commitments [Online]; 2017. Available: https://unece.org/DAM/env/documents/2017/AIR/Gothenburg%5FProtocol/Annex%5FII%5Fand%5FIII%5Fupdated%5Fclean.pdf [Accessed 9-11-21].

[13] Richmond B, Misra A, Brown P, Karagianni E, et al. UK Informative Inventory Report (1990 to 2018); 2020. Available: https://uk-air.defra.gov.uk/assets/documents/reports/cat07/2003131327_GB_IIR_2020_v1.0.pdf [Accessed 11-04-2022].

[14] Marais EA, Pandey AK, Van Damme M, Clarisse L, et al. UK ammonia emissions estimated with satellite observations and GEOS-Chem. J Geophys Res-Atmos 2021;126. https://doi.org/10.1029/2021jd035237.

[15] Lelieveld J, Evans JS, Fnais M, Giannadaki D, et al. The contribution of outdoor air pollution sources to premature mortality on a global scale. Nature 2015;525:367–71. https://doi.org/10.1038/nature15371.

[16] Pozzer A, Tsimpidi AP, Karydis VA, de Meij A, et al. Impact of agricultural emission reductions on fine-particulate matter and public health. Atmos Chem Phys 2017;17:12813–26. https://doi.org/10.5194/acp-17-12813-2017.

[17] Gu B, Zhang L, Van Dingenen R, Vieno M, et al. Abating ammonia is more cost-effective than nitrogen oxides for mitigating $PM_{2.5}$ air pollution. Science 2021;374:758–62. https://doi.org/10.1126/science.abf8623.

[18] Jonson JE, Gauss M, Schulz M, Jalkanen J-P, et al. Effects of global ship emissions on European air pollution levels. Atmos Chem Phys 2020;20:11399–422. https://doi.org/10.5194/acp-20-11399-2020.

[19] Wang QQ, Gu JW, Wang XR. The impact of Sahara dust on air quality and public health in European countries. Atmos Environ 2020;241:10. https://doi.org/10.1016/j.atmosenv.2020.117771.

[20] Harrison RM, Van Vu T, Jafar H, Shi ZB. More mileage in reducing urban air pollution from road traffic. Environ Int 2021;149:8. https://doi.org/10.1016/j.envint.2020.106329.

[21] Fuller GW, Tremper AH, Baker TD, Yttri KE, et al. Contribution of wood burning to PM$_{10}$ in London. Atmos Environ 2014;87:87–94. https://doi.org/10.1016/j.atmosenv.2013.12.037.

[22] DEFRA. Emissions of air pollutants in the UK – Particulate matter (PM$_{10}$ and PM$_{2.5}$) [Online]; 2022. Available: https://www.gov.uk/government/statistics/emissions-of-air-pollutants/emissions-of-air-pollutants-in-the-uk-particulate-matter-pm10-and-pm25 [Accessed 12-04-2022].

[23] City Mayors Statistics. The UK's 200 largest towns, cities and districts [Online]; 2010. Available: http://www.citymayors.com/gratis/uk_topcities.html [Accessed 11-04-2022].

[24] Leicester City Council. 2014. Healthier Air for Leicester, Leicester's Air Quality Action Plan (2015-2026). Available: https://www.leicester.gov.uk/media/180653/air-quality-action-plan.pdf [Accessed 11-04-2022].

[25] Potts DA, Marais EA, Boesch H, Pope RJ, et al. Diagnosing air quality changes in the UK during the COVID-19 lockdown using TROPOMI and GEOS-Chem. Environ Res Lett 2021;16. https://doi.org/10.1088/1748-9326/abde5d.

[26] Department for Transport & Office of National Statistics. Transport use during the coronavirus (COVID-19) pandemic [Online]; 2022. Available: https://www.gov.uk/government/statistics/transport-use-during-the-coronavirus-covid-19-pandemic [Accessed 12-04-2022].

[27] Marais EA, Jacob DJ, Turner JR, Mickley LJ. Evidence of 1991–2013 decrease of biogenic secondary organic aerosol in response to SO$_2$ emission controls. Environ Res Lett 2017;12. https://doi.org/10.1088/1748-9326/aa69c8.

[28] Qu Z, Jacob DJ, Silvern RF, Shah V, et al. US COVID-19 shutdown demonstrates importance of background NO$_2$ in inferring NO$_x$ emissions from satellite NO$_2$ observations. Geophys Res Lett 2021;48. https://doi.org/10.1029/2021gl092783.

[29] Bouwman AF, Lee DS, Asman WAH, Dentener FJ, et al. A global high-resolution emission inventory for ammonia. Global Biogeochem Cycles 1997;11:561–87. https://doi.org/10.1029/97gb02266.

[30] Riddick SN, Dragosits U, Blackall TD, Daunt F, et al. The global distribution of ammonia emissions from seabird colonies. Atmos Environ 2012;55:319–27. https://doi.org/10.1016/j.atmosenv.2012.02.052.

[31] Guenther AB, Jiang X, Heald CL, Sakulyanontvittaya T, et al. The Model of Emissions of Gases and Aerosols from Nature version 2.1 (MEGAN2.1): an extended and updated framework for modeling biogenic emissions. Geosci Model Dev 2012;5:1471–92. https://doi.org/10.5194/gmd-5-1471-2012.

[32] Fairlie TD, Jacob DJ, Park RJ. The impact of transpacific transport of mineral dust in the United States. Atmos Environ 2007;41:1251–66. https://doi.org/10.1016/j.atmosenv.2006.09.048.

[33] Jaeglé L, Quinn PK, Bates TS, Alexander B, et al. Global distribution of sea salt aerosols: new constraints from in situ and remote sensing observations. Atmos Chem Phys 2011;11:3137–57. https://doi.org/10.5194/acp-11-3137-2011.

[34] Park RJ, Jacob DJ, Field BD, Yantosca RM, et al. Natural and transboundary pollution influences on sulfate-nitrate-ammonium aerosols in the United States: Implications for policy. J Geophys Res-Atmos 2004;109:20. https://doi.org/10.1029/2003jd004473.

[35] Pai SJ, Heald CL, Pierce JR, Farina SC, et al. An evaluation of global organic aerosol schemes using airborne observations. Atmos Chem Phys 2020;20:2637–65. https://doi.org/10.5194/acp-20-2637-2020.

[36] Silvern RF, Jacob DJ, Kim PS, Marais EA, et al. Inconsistency of ammonium-sulfate aerosol ratios with thermodynamic models in the eastern US: a possible role of organic aerosol. Atmos Chem Phys 2017;17:5107–18. https://doi.org/10.5194/acp-17-5107-2017.

[37] Nault BA, Campuzano-Jost P, Day DA, Jo DS, et al. Chemical transport models often underestimate inorganic aerosol acidity in remote regions of the atmosphere. Commun Earth Environ 2021;2. https://doi.org/10.1038/s43247-021-00164-0.

[38] Fountoukis C, Nenes A. ISORROPIA II: a computationally efficient thermodynamic equilibrium model for K$^+$-Ca^{2+}-Mg^{2+}-NH$_4^+$-Na$^+$-SO$_4^{2-}$-NO$_3^-$-Cl$^-$-H$_2$O aerosols. Atmos Chem Phys 2007;7:4639–59. https://doi.org/10.5194/acp-7-4639-2007.

[39] Cooke WF, Liousse C, Cachier H, Feichter J. Construction of a 1° × 1° fossil fuel emission data set for carbonaceous aerosol and implementation and radiative impact in the ECHAM4 model. J Geophys Res Atmos 1999;104:22137–62. https://doi.org/10.1029/1999jd900187.

[40] Wesely ML. Parameterization of surface resistances to gaseous dry deposition in regional-scale numerical models. Atmos Environ 1989;23:1293–304. https://doi.org/10.1016/0004-6981(89)90153-4.

[41] Zhang LM, Gong SL, Padro J, Barrie L. A size-segregated particle dry deposition scheme for an atmospheric aerosol module. Atmos Environ 2001;35:549–60. https://doi.org/10.1016/s1352-2310(00)00326-5.

[42] Liu HY, Jacob DJ, Bey I, Yantosca RM. Constraints from Pb-210 and Be-7 on wet deposition and transport in a global three-dimensional chemical tracer model driven by assimilated meteorological fields. J Geophys Res-Atmos 2001;106:12109–28. https://doi.org/10.1029/2000jd900839.

[43] Amos HM, Jacob DJ, Holmes CD, Fisher JA, et al. Gas-particle partitioning of atmospheric Hg$_{(II)}$ and its effect on global mercury deposition. Atmos Chem Phys 2012;12:591–603. https://doi.org/10.5194/acp-12-591-2012.

[44] Butterfield D, Quincey P. NPL REPORT AS 15, Measurement science issues relating to PM$_{10}$ and PM$_{2.5}$ airborne particles; 2007. Available: https://eprintspublications.npl.co.uk/4023/1/AS15.pdf [Accessed 11-04-2022].

[45] Turpin BJ, Lim H-J. Species contributions to PM$_{2.5}$ mass concentrations: Revisiting common assumptions for estimating organic mass. Aerosol Sci Tech 2001;35:602–10. https://doi.org/10.1080/02786820119445.

[46] Vieno M, Heal MR, Williams ML, Carnell EJ, et al. The sensitivities of emissions reductions for the mitigation of UK PM$_{2.5}$. Atmos Chem Phys 2016;16:265–76. https://doi.org/10.5194/acp-16-265-2016.

[47] Philip S, Martin RV, Snider G, Weagle CL, et al. Anthropogenic fugitive, combustion and industrial dust is a significant, underrepresented fine particulate matter source in global atmospheric models. Environ Res Lett 2017;12:7. https://doi.org/10.1088/1748-9326/aa65a4.

[48] Caiazzo F, Ashok A, Waitz IA, Yim SHL, et al. Air pollution and early deaths in the United States. Part I: Quantifying the impact of major sectors in 2005. Atmos Environ 2013;79:198–208. https://doi.org/10.1016/j.atmosenv.2013.05.081.

[49] Liu J, Mauzerall DL, Chen Q, Zhang Q, et al. Air pollutant emissions from Chinese households: A major and underappreciated ambient pollution source. Proc Natl Acad Sci 2016;113:7756–61. https://doi.org/10.1073/pnas.1604537113.

[50] Marais EA, Silvern RF, Vodonos A, Dupin E, et al. Air quality and health impact of future fossil fuel use for electricity generation and transport in Africa. Environ Sci Tech 2019;53:13524–34. https://doi.org/10.1021/acs.est.9b04958.

[51] Bockarie AS, Marais EA, MacKenzie AR. Air pollution and climate forcing of the charcoal industry in Africa. Environ Sci Tech 2020;54:13429–38. https://doi.org/10.1021/acs.est.0c03754.

[52] McDuffie EE, Martin RV, Spadaro JV, Burnett R, et al. Source sector and fuel contributions to ambient PM$_{2.5}$ and attributable mortality across multiple spatial scales. Nat Commun 2021;12. https://doi.org/10.1038/s41467-021-23853-y.

[53] Thunis P, Clappier A, Pisoni E, Degraeuwe B. Quantification of non-linearities as a function of time averaging in regional air quality modeling applications. Atmos Environ 2015;103:263–75. https://doi.org/10.1016/j.atmosenv.2014.12.057.

[54] Tang YS, Braban CF, Dragosits U, Simmons I, et al. Acid gases and aerosol measurements in the UK (1999–2015): regional distributions and trends. Atmos Chem Phys 2018;18:16293–324. https://doi.org/10.5194/acp-18-16293-2018.

[55] Beccaceci, S., Mcghee, E., Robins, C., Butterfield, D., et al. 2015. Airborne Particulate Concentrations and Numbers in the United Kingdom (phase 3), Annual report 2015. Available: https://uk-air.defra.gov.uk/assets/documents/reports/cat09/1807161507_Particles_Network_Annual_Report_2015.pdf [Accessed 25-04-2022].

[56] Hagan DH, Kroll JH. Assessing the accuracy of low-cost optical particle sensors using a physics-based approach. Atmos Meas Tech 2020;13:6343–55. https://doi.org/10.5194/amt-13-6343-2020.

[57] Crilley LR, Shaw M, Pound R, Kramer LJ, et al. Evaluation of a low-cost optical particle counter (Alphasense OPC-N2) for ambient air monitoring. Atmos Meas Tech 2018;11:709–20. https://doi.org/10.5194/amt-11-709-2018.

[58] Tryner J, L'Orange C, Mehaffy J, Miller-Lionberg D, et al. Laboratory evaluation of low-cost PurpleAir PM monitors and in-field correction using co-located portable filter samplers. Atmos Environ 2020;220. https://doi.org/10.1016/j.atmosenv.2019.117067.

[59] Nilson B, Jackson PL, Schiller CL, Parsons MT. Development and evaluation of correction models for a low-cost fine particulate matter monitor. Atmos Meas Tech 2022;15:3315–28. https://doi.org/10.5194/amt-15-3315-2022.

[60] Mircea M, Bessagnet B, D'Isidoro M, Pirovano G, et al. EURODELTA III exercise: An evaluation of air quality models' capacity to reproduce the carbonaceous aerosol. Atmos Environ-X 2019;2. https://doi.org/10.1016/j.aeaoa.2019.100018.

[61] Wang Q, Jacob DJ, Spackman JR, Perring AE, et al. Global budget and radiative forcing of black carbon aerosol: Constraints from pole-to-pole (HIPPO) observations across the Pacific. J Geophys Res Atmos 2014;119:195–206. https://doi.org/10.1002/2013jd020824.

[62] Hellsten S, Dragosits U, Place CJ, Vieno M, et al. Modelling the spatial distribution of ammonia emissions in the UK. Environ Pollut 2008;154:370–9. https://doi.org/10.1016/j.envpol.2008.02.017.

[63] Harrison RM, Laxen D, Moorcroft S, Laxen K. Processes affecting concentrations of fine particulate matter (PM$_{2.5}$) in the UK atmosphere. Atmos Environ 2012;46:115–24. https://doi.org/10.1016/j.atmosenv.2011.10.028.

[64] Fenech S, Doherty RM, Heaviside C, Macintyre HL, et al. Meteorological drivers and mortality associated with O$_3$ and PM$_{2.5}$ air pollution episodes in the UK in 2006. Atmos Environ 2019;213:699–710. https://doi.org/10.1016/j.atmosenv.2019.06.030.

[65] Kim PS, Jacob DJ, Fisher JA, Travis K, et al. Sources, seasonality, and trends of southeast US aerosol: an integrated analysis of surface, aircraft, and satellite observations with the GEOS-Chem chemical transport model. Atmos Chem Phys 2015;15:10411–33. https://doi.org/10.5194/acp-15-10411-2015.

[66] Kendon M, McCarthy M, Jevrejeva S, Matthews A, et al. State of the UK climate 2019. Int J Climatol 2020;40. https://doi.org/10.1002/joc.6726.

[67] Department for Transport. The Merchant Shipping (Prevention of Air Pollution from Ships) (Amendment) Regulations 2021; 2020. Available: https://assets.publishing.service.gov.uk/government/uploads/system/uploads/attachment_data/file/989793/draft-impact-assessment-merchant-shipping-regulations-2021.pdf [Accessed 11-04-2022].